Neutron-scattering profile of $Q \neq 0$ phonons in BCS superconductors

Philip B. Allen and Vladimir N. Kostur
Department of Physics and Astronomy, State University of New York, Stony Brook, New York 11794-3800

Naohisa Takesue
ISSP, Neutron Scattering Laboratory, University of Tokyo, Tokai, Ibaraki 319-11, Japan

Gen Shirane
Department of Physics, Brookhaven National Laboratory, Upton, New York 11973
(Received 15 April 1997)

Phonons in a metal interact with conduction electrons. In the normal state, this gives rise to a linewidth γ_Q which is small compared with the frequency ω_Q. In the superconducting state, the line shape can be altered if $\hbar\omega_Q \lesssim (1+2r)2\Delta$ where Δ is the superconducting gap, and r is the ratio γ_Q/ω_Q, which scales with the strength of the electron-phonon coupling λ. As long as $\omega_Q \ll Qv_F$ where v_F is the Fermi velocity, BCS theory predicts a line shape which is a universal function of the dimensionless parameters r, $\omega_Q/2\Delta$, $\omega/2\Delta$, and T/T_c where T_c is the superconducting transition temperature. Formulas and curves are given for the full range of these parameters. The BCS predictions correspond well to key features seen in recent experiments on YNi_2B_2C and $LuNi_2B_2C$. [S0163-1829(97)05033-9]

I. INTRODUCTION

The recently discovered superconducting compounds $Ln Ni_2B_2C$ (where Ln is Y, Lu, etc.) are the first materials to show a dramatic alteration of phonon line shape when temperature T is reduced below the transition temperature T_c. This has been seen by Kawano *et al.*[1] and by Stassis *et al.*[2] using neutron scattering. Shapiro *et al.*[3] did early neutron studies of changes in the phonon line shapes in the conventional superconducting metal Nb. Several groups[4,5] measured an effect in high-T_c compounds by neutron scattering.

There are many measurements for infrared and Raman-active phonons in high-T_c superconductors.[6–9] Observed phonon peaks broaden or narrow, and shift up or down in frequency depending on the phonon position relative to the superconducting gap 2Δ. Theories for optical phonons were proposed by Klein and Dierker[10] within BCS theory and Zeyher and Zwicknagl[11] within Eliashberg theory. The latter theory gives remarkable agreement with experimental data.[7]

Unlike infrared and Raman, neutron experiments access $\mathbf{Q} \neq \mathbf{0}$ phonons. Even though the theory is simplified by the fact that that impurity scattering plays no role for $Q\ell \gg 1$ (where ℓ is the electron mean free path), nevertheless theoretical discussions are fewer. Representative experimental results for $Ln Ni_2B_2C$ are shown in Fig. 1. Because the line shapes are unusual looking, various interesting interpretations have been proposed.[1,2,12] Several papers have calculated line shapes for $\mathbf{Q} \neq \mathbf{0}$ phonons,[13,14] but the simple predictions of orthodox BCS theory still need clarification and testing. The present paper gives the predictions and suggests the appropriate tests for $\mathbf{Q} \neq \mathbf{0}$ phonons.

II. THEORY

Assuming that the sample is well ordered and reasonably harmonic so that well-defined phonon peaks exist, the neutron-scattering profile $S(Q,\omega)$ of a phonon is approximately the imaginary part of the phonon Green's function

$$S(Q,\omega) = -\mathrm{Im}\left\{\frac{1}{(\omega^2-\omega_Q^2)/2\omega_Q - \delta\Pi(Q,\omega)}\right\}. \quad (1)$$

As explained in Appendix A, $\delta\Pi(Q,\omega)$ contains the imaginary part of the phonon self-energy in the N-state, plus (in the S-state) the shift in the phonon self-energy caused by superconductivity. An elementary theory for the imaginary

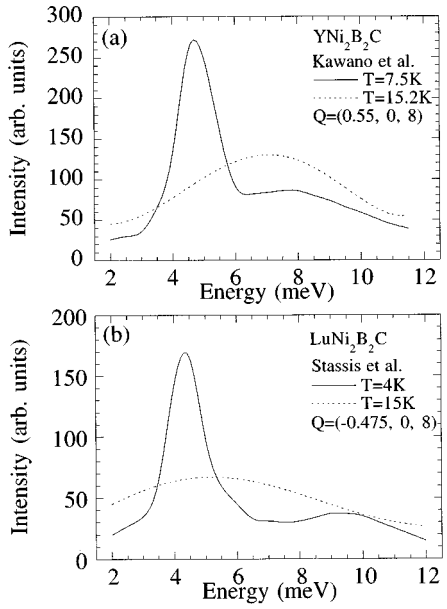

FIG. 1. Schematic representation of phonon line shapes in the superconducting (solid line) and normal (dashed line) states observed by inelastic neutron-scattering experiments on (a) YNi_2B_2C (Ref. 1) and (b) $LuNi_2B_2C$ (Ref. 2), respectively.

part of the self-energy is given in Appendixes B and C. In the N-state, the result is Eq. (A4).

A. Imaginary part of phonon self-energy

From Eq. (C4) the BCS result for the imaginary part of the phonon self-energy can be written

$$-\mathrm{Im}[\Pi_S(Q,\omega)]=\frac{r_Q}{2}\int_{-\infty}^{\infty}d\epsilon\int_{-\infty}^{\infty}d\epsilon'\left\{\left(1+\frac{\epsilon\epsilon'-\Delta(T)^2}{EE'}\right)\times[f(E)-f(E')]\delta(E'-E-\omega)+\frac{1}{2}\left(1-\frac{\epsilon\epsilon'-\Delta(T)^2}{EE'}\right)[1-f(E)-f(E')]\delta(E'+E-\omega)\right\},\tag{2}$$

where E is $\sqrt{\epsilon^2+\Delta(T)^2}$, $\Delta(T)$ is the T-dependent BCS gap, and $f(E)$ is the Fermi-Dirac function $1/[\exp(E/k_BT)+1]$. We have used the approximate Clem[15] formula for the BCS gap, rather than solving the BCS gap equation. Equation (2) agrees with formulas found in the literature, for example, Ref. 16. The imaginary part of the phonon correlation function depends only upon the dimensionless parameters $\omega/2\Delta$, $\omega_Q/2\Delta$, T/T_c, and $r_Q\equiv\gamma_Q/\omega_Q$, where γ_Q is the normal-state half-width at half maximum of the phonon line, given by Eq. (B4). This last is just a multiplicative scale factor.

To evaluate Eq. (2) numerically, it is convenient to make some variable transformations. We have split it into two parts, $-\mathrm{Im}[\Pi_S(Q,\omega)]/\gamma_Q=(\omega/\omega_Q)(r_1+r_2)$,

$$r_1=\int_0^{\pi/2}\frac{d\theta}{\sin^2\theta}\frac{1+\nu\sin\theta-\sin^2\theta}{\sqrt{(1+\nu\sin\theta)^2-\sin^2\theta}}\times\left[f\left(\frac{\beta\Delta(T)}{\sin\theta}\right)-f\left(\beta\omega+\frac{\beta\Delta(T)}{\sin\theta}\right)\right],\tag{3}$$

$$r_2=\int_0^{\pi/2}d\theta\frac{(1-a)+\frac{1}{2}a^2\cos^2\theta}{\sqrt{(1-a)+\frac{1}{4}a^2\cos^2\theta}}\left[1-f\left(\frac{\beta\omega}{2}(1+a\sin\theta)\right)-f\left(\frac{\beta\omega}{2}(1-a\sin\theta)\right)\right]\theta(\omega-2\Delta(T)),\tag{4}$$

where ν is $\omega/\Delta(T)$, β is k_BT, and a is $1-2\Delta(T)/\omega$. The function $\theta(a)$ is the usual unit step. In Fig. 2, we have evaluated Eq. (2) for several values of T/T_c and plotted it versus $\omega/2\Delta$. Notice that there is a discontinuity at the frequency $\omega=2\Delta(T)$ where pairs can first be broken. The size of the step is fixed by the value of r_2 at $a=0$, namely $(\pi/2)\tanh(\Delta(T)/2T)$, which shrinks to zero size and moves to zero frequency as $T\to T_c$.

Another important feature of Eq. (2) is the high-frequency limit. At $T=0$, we found the result

$$-\mathrm{Im}[\Pi_S(Q,\omega)]\approx r_Q\omega\left\{1+\frac{1}{2}\left(\frac{2\Delta}{\omega}\right)^2\left[\ln\left(\frac{2\omega}{\Delta}\right)-\frac{1}{2}\right]+\cdots\right\}.\tag{5}$$

We did not find a simple derivation, nor an answer when $T>0$. This gives such an accurate fit to numerical results (at $\omega/2\Delta$ greater than ≈ 25) that we believe the first correction term is at most $(2\Delta/\omega)^4$ times a logarithm.

The strength of the electron-phonon coupling enters the theory through the dimensionless ratio γ_Q/ω_Q. One of us[17] has shown that the average value of this ratio (averaged over the whole phonon spectrum) has the value

$$\langle r\rangle=(\gamma/\omega)_{\mathrm{ave}}=\frac{\pi}{6}N(0)\hbar\langle\omega\rangle\lambda,\tag{6}$$

where $N(0)$ is the electron density of states (per spin and per atom), λ is the mass enhancement parameter which approximately determines T_c, and $\langle\omega\rangle$ is an average vibrational frequency. To get a reasonably large value for the parameter r_Q, it is therefore helpful to have a material with large values of $N(0)$ and $\langle\omega\rangle$. Metallic Nb has reasonably large values for both, which give $\langle r\rangle\approx 0.01$. This is also approximately the size seen in the neutron measurement of Shapiro *et al.*[3] Band theory gives values of $N(0)$ for $LuNi_2B_2C$ comparable to Nb on a per atom basis.[18] It is not likely to find values of $\langle r\rangle$ too much larger than this in any stable

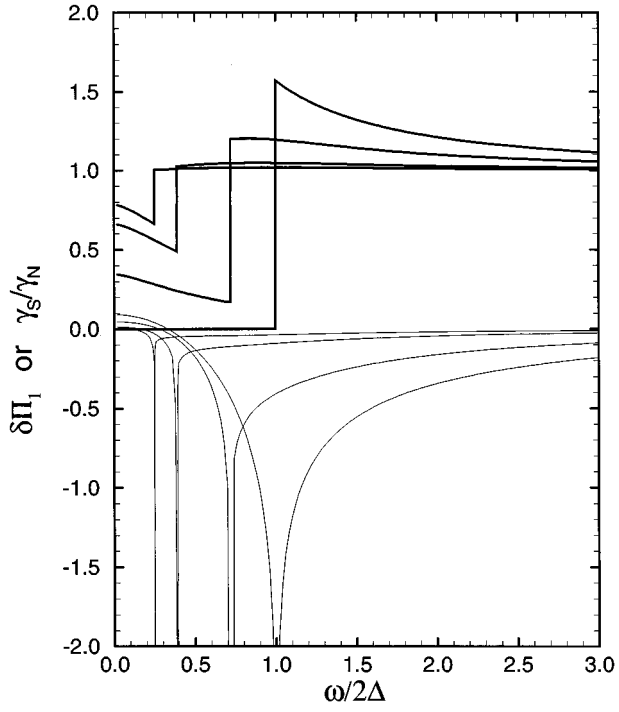

FIG. 2. Bold curves are γ_S/γ_N (ratio of superconducting to normal values of the imaginary part of the phonon self-energy) shown at four temperatures ($T=0$, $0.8T_c$, $0.95T_c$, and $0.98T_c$). Light curves are $\delta\Pi_1/\gamma_N$ (difference between superconducting and normal values of the real part of the phonon self-energy divided by the normal-state imaginary part) shown at the same four temperatures.

metal, but individual branches of the spectrum are permitted to have much larger values of r_Q.

B. Real part of phonon self-energy

In the normal state, the real part is defined to be absorbed into the ''unperturbed'' Green's function $D^{-1}=(\omega^2-\omega_Q^2)/2\omega_Q$ by use of experimental rather than bare phonon frequencies. Thus, in the N-state, $\delta\Pi(Q,\omega)$ is set equal to the imaginary part, $-ir_Q\omega$. However, in the S-state, the difference $\Pi_S-\Pi_N$ has a real part, and this must be used for the real part of $\delta\Pi(Q,\omega)$. We compute this by Kramers-Kronig analysis of the imaginary part of $\Pi_S-\Pi_N$,

$$\mathrm{Re}\{\delta\Pi(q,\omega)\}=\frac{P}{\pi}\int_0^\infty d\omega'\,\frac{2\omega'[\mathrm{Im}\{\Pi_S(Q,\omega')\}+r_Q\omega']}{\omega'^2-\omega^2}. \tag{7}$$

At large ω', the integrand of Eq. (7) goes like $\log(\omega')/\omega'^2$ [using Eq. (5)], so the integration converges rather slowly. To be safe, we integrated up to $\omega'/2\Delta=1000$. Results for the real part are also shown in Fig. 2. Notice that the discontinuity in the imaginary part at $\omega=2\Delta(T)$ generates a logarithmic singularity in the real part at the same value of ω. These singularities persist up to $T=T_c$, but get smaller and move to lower ω.

III. NUMERICAL RESULTS

Phonon profiles have been computed numerically using Eqs. (1),(2),(3),(4),(7) above. To be explicit, the formula is

$$S(Q,\omega)=\frac{4\omega r_Q\omega_Q^2\gamma_S/\gamma_N}{[\omega^2-\omega_Q^2-2\omega_Q^2 r_Q\mathrm{Re}(\delta\Pi)/\gamma_N]^2+[2\omega r_Q\omega_Q\gamma_S/\gamma_N]^2}, \tag{8}$$

where γ_S is $-\mathrm{Im}\delta\Pi_S(Q,\omega)$ and γ_N is γ_Q. In addition to the dimensionless parameters of the theory, ω_Q [measured from now on in units of $2\Delta=2\Delta(0)$], $t=T/T_c$, and $r\equiv\gamma_Q/\omega_Q$, we use also a parameter Γ (also measured in units of 2Δ) to represent experimental resolution broadening. As a test of this formula we fitted the data of Shapiro *et al.*[3] for Nb. The parameters $2\Delta_0=3.1$ meV, $r_Q=0.01$, and $\Gamma=0.03$ gave a completely satisfactory fit to the data of Fig. 3 of Ref. 3. The parameter $r_Q=0.01$ agrees with earlier qualitative conclusions made without curve fitting,[17] and also agrees with first-principles calculations of electron-phonon coupling in Nb,[19] and neutron measurements of the dispersion of γ_Q in the normal state.[19] We examine the results for the full range of $t<1$ and ω_Q. The other two variables are assigned values appropriate to recent measurements. The value of r is chosen to be 0.30 because the experimental spectrum[1] [shown in Fig. 1(a)] has a half-width ≈ 2.5 meV and a peak frequency ≈ 7 meV in the N-state. Two values of Γ have been used, $\Gamma=0$ and $\Gamma=0.13$, which corresponds to 0.5 meV instrumental half-width if the value of 2Δ is 4 meV.

Figure 3 illustrates how the phonon profile varies at a low T ($t=0.2$) in the S-state and in the (T-independent) N state, when the phonon energy ω_Q is varied from below to above $2\Delta(T)$, without and with additional broadening from instrumental resolution. The unconvoluted S-state spectra show a sharp peak below $2\Delta(T)$ and a broad peak above $2\Delta(T)$, whereas the N-state spectra just have a single broad peak. When $\omega_Q<2\Delta(T)$, [Fig. 3(a)] the sharp peak below $\omega=2\Delta(T)$ contains most of the weight and represents a phonon with enhanced lifetime because electronic decay channels are frozen out by the superconducting gap. The component of the N-state phonon line which lies above $2\Delta(T)$ in the S-state is less affected by superconductivity, but has its spectral weight somewhat altered for ω just above $2\Delta(T)$ for reasons which are a complicated mixture of superconducting density-of-states effects, coherence effects, and renormalization effects (from the real part of $\delta\Pi_S$.) The total spectral weight is conserved. When the N-state phonon has $\omega_Q>2\Delta(T)$ [Figs. 3(b) and 3(c)], the sharp feature pinned at ω just below $2\Delta(T)$ has a less intuitive explanation. The logarithmic singularity of $\mathrm{Re}\{\delta\Pi_S\}$ guarantees that the denominator of $S(Q,\omega)$, Eq. (1), always has a vanishing real part for some frequency $\omega<2\Delta(T)$, and at low T, the imaginary part is also small, so a resonance occurs. Under the right conditions (ω_Q within r of 1 and t low) this resonance captures a lot of the spectral weight. For higher ω_Q, the spectral weight returns mostly to the original phonon resonance. The resonance below $2\Delta(T)$ can be regarded as a mixed vibrational/superelectronic collective excitation, and was noticed by Schuster.[13]

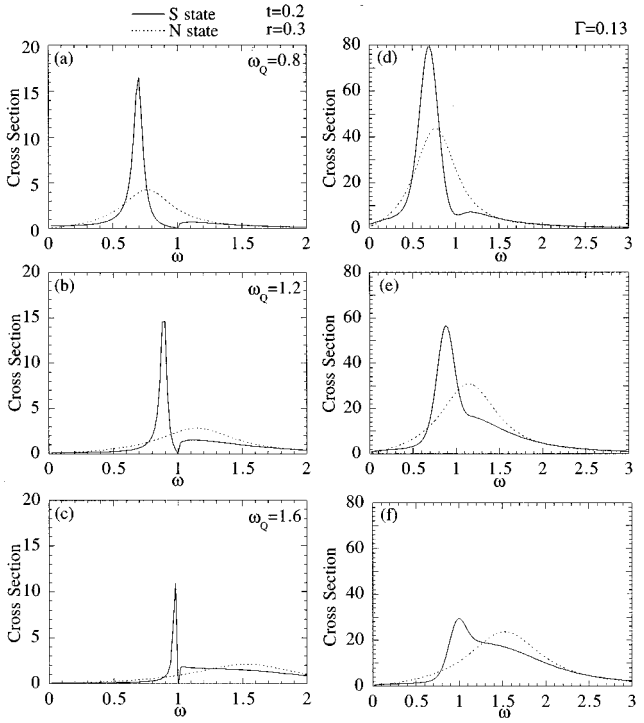

FIG. 3. Calculated line shapes at $\omega_Q=$ (a) 0.8, (b) 1.2, and (c) 1.6 (units of 2Δ) at $T/T_c=t=0.2$. Panels (d)–(f) are convoluted with an instrumental broadening $\Gamma=0.13$ (units of 2Δ).

Figure 4 shows the temperature dependence of the line shapes at $\omega_Q=0.8$ at $t=0.4$, 0.7, and 0.995. As temperature increases, the resonance below $2\Delta(T)$ broadens (because of damping by thermally excited electronic quasiparticles) and

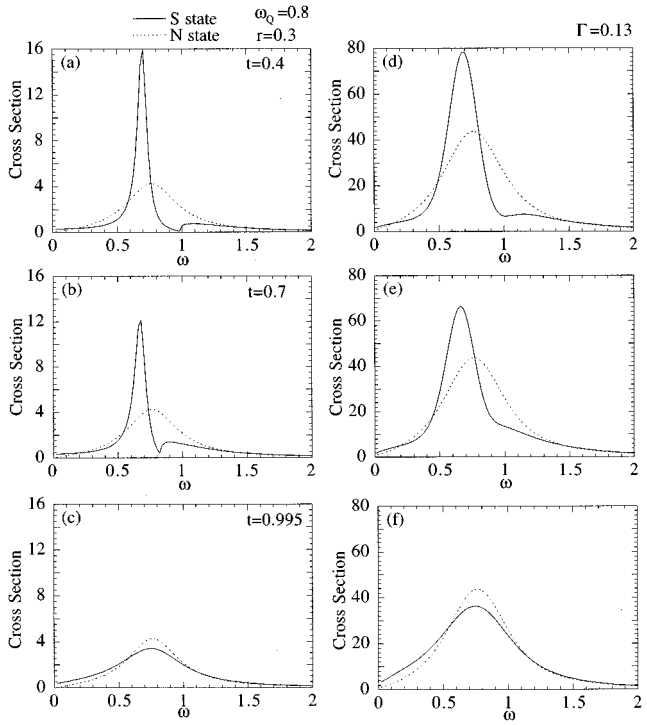

FIG. 4. Calculated line shapes at $t=$ (a) 0.4, (b) 0.7, and (c) 0.995 for $\omega_Q=0.8$. Panels (d)–(f) are broadened by $\Gamma=0.13$.

loses spectral weight to broad component above $2\Delta(T)$ [because $\Delta(T)$ is diminished]. Similar effects are shown in Fig. 5 for a phonon with $\omega_Q=1.2$. The sharp component shifts downward as T increases and $\Delta(T)$ decreases, but by the time $\Delta(T)$ has diminished a lot, the damping has almost restored a N-state line shape and the sharp peak disappears.

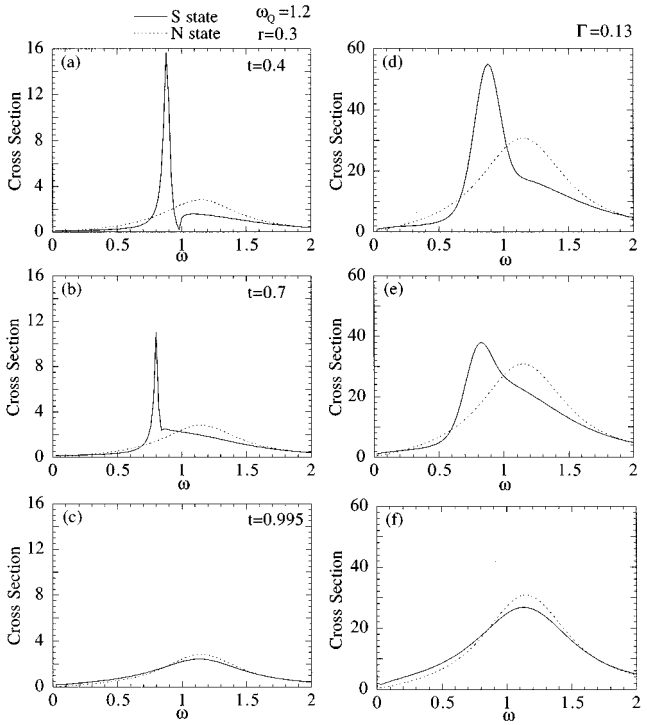

FIG. 5. Calculated line shapes at $t=$ (a) 0.4, (b) 0.7, and (c) 0.995 for $\omega_Q=1.2$. Panels (d)–(f) are broadened by $\Gamma=0.13$.

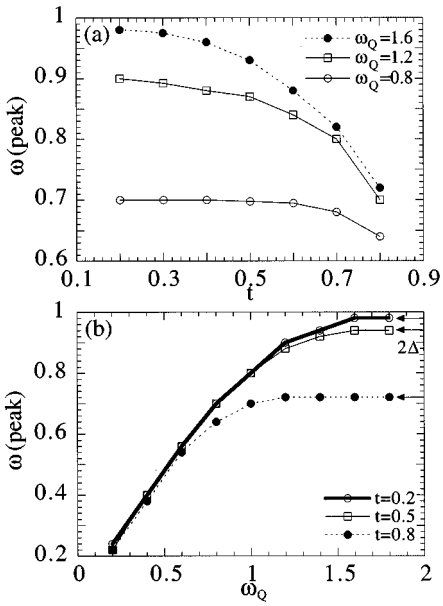

FIG. 6. Dependences of the sharp resonance frequency on (a) t and (b) ω_Q. Arrows indicate the gap energy $2\Delta(T)$ at each temperature.

Figure 6 shows the behavior of the position of the sharp peak below $2\Delta(T)$ for all frequencies ω_Q and all temperature, using unbroadened line shapes. The following seem to be the key indicators of canonical BCS behavior:

(1) At $t>0.5$, phonons with $\omega_Q>0.8$ have a significant temperature shift of the sharp resonance.

(2) There is almost no t dependence of the peak position for $t<0.5$ or $\omega_Q<0.8$.

(3) For $\omega_Q<0.8$, the dispersion of the sharp peak with Q is close to the normal-state dispersion.

(4) For $\omega_Q>1.2$, the sharp peak is pinned just below $2\Delta(T)$ and shows no more dispersion with Q.

IV. COMPARISON WITH EXPERIMENT

The overall appearance of the instrumentally broadened BCS line shapes shown in Figs. 3–5 resemble nicely the experimental profiles as shown in Fig. 1. Therefore it might not be necessary to invoke ''new excitations'' as suggested by Kawano *et al.*[1] to explain the data. Our results lend some support to the ''decoupled TA mode'' interpretation of Stassis *et al.*[2]

The results of the previous neutron studies[1,2] show no temperature dependence of the sharp peak frequency, but exhibit dispersion as Q is varied. This suggests that the N-state frequency might lie in the range $\omega_Q<0.8$ shown in Fig. 6(b). If the measurement is performed at a different Q with $\omega_Q>1.2$ (the range where dispersion is predicted to disappear), then our calculations show that orthodox BCS theory predicts that the sharp peak should be pinned and diminish in frequency as T increases and $2\Delta(T)$ decreases.

The calculation by Kee and Varma[12] differs from ours because they have assumed that the phonon under consideration is ''extremal'' on the Fermi surface, in a well-defined sense, which enhances both the N-state and the S-state self-energy effects. Our work indicates that it may not be necessary to invoke this special feature. The experimental signa-

ture of the Kee-Varma scenario should be a rapid disappearance of the anomalous line shapes as the wave vector is varied, whereas the canonical BCS behavior is predicted to vary more smoothly.

Further experiment should test the BCS picture in some detail. In order to do this in $LnNi_2B_2C$, it will be necessary to measure 2Δ more accurately. Gap energies determined so far[20–23] distribute from 4 to 7 meV. However, the temperature dependence of $\Delta(T)$ was established to be BCS-like in a recent experiment,[23] which strengthens our view that canonical BCS behavior explains the observations.

ACKNOWLEDGMENTS

We thank C. Stassis, S. M. Shapiro, M. Bullock, and C. M. Varma for stimulating comments. N.T. thanks Y. Fujii for sponsorship. This work was supported by NSF Grant No. DMR-9417755, by the U.S.-Japan Cooperative Research Program on Neutron Scattering, and by the U.S. DOE Contract No. DE-AC02-76CH00016.

APPENDIX A: FRÖHLICH HAMILTONIAN

The Fröhlich Hamiltonian simplifies the problem by omitting Coulomb interactions between electrons. Although not a full theory, this is sufficient to contain the change of phonon properties caused by superconductivity, as explained below. The Hamiltonian is

$$H=\sum_k \epsilon_k c_k^\dagger c_k+\sum_Q \omega_Q a_Q^\dagger a_Q+\sum_{k,k'} M_{k,k'} c_{k'}^\dagger c_k (a_Q+a_{-Q}^\dagger), \tag{A1}$$

where ϵ_k is the energy of the electron state labeled by quantum numbers k, ω_Q is the energy of the phonon state labeled by quantum numbers Q, and $M_{k,k'}$ is the screened matrix element coupling electrons to phonons. The wave vector of the electrons ($\vec{k}$, $\vec{k}'$) and of the phonon ($\vec{Q}$) must obey the usual $\vec{k}$-conservation *modulo* a reciprocal-lattice vector. A full theory would use, instead of $M_{k,k'}$, a bare matrix element $g_{k,k'}$, and would have in addition a Coulomb interaction term between electrons. This theory would then be used to calculate the phonon Green's function D and self-energy Π, related by the Dyson equation $D^{-1}=D_0^{-1}-\Pi$ to the bare Green's function D_0 calculated without coupling to electrons. Impurity scattering is also omitted. This is valid as long as $Q\ell \gg 1$ where Q is the wave vector of the experiment and ℓ is the electron mean free path at the Fermi energy.

By a standard analysis of perturbation theory, the self-energy is

$$\Pi=g^2\chi/(1+v\chi), \tag{A2}$$

where v is the matrix element of the Coulomb interaction, and χ is the irreducible polarizability. The neutron-scattering profile is proportional to the imaginary part of D, and is needed only near the resonance at $\omega\approx\omega_Q$. In this low-ω region, in the normal state, the real part of Π is large and ω independent, while the imaginary part of Π is small and ω dependent. It is then appropriate to incorporate the real part of Π into the Green's function, now called D_1, and equal to $2\omega_Q/(\omega^2-\omega_Q^2)$, leaving as the residual self-energy, $\delta\Pi$, just the small imaginary part:

$$D^{-1}(Q,\omega)=(\omega^2-\omega_Q^2)/2\omega_Q-\delta\Pi(Q,\omega). \tag{A3}$$

In the normal (N) state, the low-energy formula for $\delta\Pi$ is

$$-\mathrm{Im}\{\delta\Pi_N\}=(\gamma_Q/\omega_Q)\omega. \tag{A4}$$

A specific form for $\gamma_Q=1/2\tau_Q$ (γ_Q is the half-width at half maximum of the phonon resonance, and $1/\tau_Q$ is the rate of relaxation of the phonon population back to equilibrium) is given in the next Appendix.

In the superconducting state, the self-energy Π_S is altered for energies $\omega\lesssim 2(1+2r)\Delta$ where $2\Delta\approx 3.52k_BT_c$ is the gap of BCS theory. The alteration replaces χ in Eq. (A2) by $\chi+\delta\chi_S$. The result is designated $\Pi+\delta\Pi_S$. Then it is easy to verify that

$$\delta\Pi_S=[g/(1+v\chi)]^2\delta\chi_S=M^2\delta\chi_S, \tag{A5}$$

where the screened matrix element $M_{k,k'}$ appearing in Eq. (A5) is the same as the one appearing in Eq. (A1). If one does perturbation theory using the Fröhlich Hamiltonian Eq. (A1), then the result agrees with Eqs. (A3) and (A5), which provide the needed justification. The neutron-scattering profile in the superconducting state is then found by using Eq. (A5) in Eq. (A3).

APPENDIX B: PHONON DECAY IN THE NORMAL STATE

Diagrammatic perturbation theory to second order in M gives the desired formulas for Π, and the imaginary part of Π gives the theory for phonon decay. An equally rigorous derivation can be made of the imaginary part by an elementary method, and then the real part can be constructed by Kramers-Kronig analysis. Since this corresponds to the computational route that we prefer, we now give the elementary derivation.

Imagine that the phonon occupation function $N(Q,r)$ is somehow out of equilibrium, but spatially homogenous so that there is no r dependence. Then the time rate of evolution of $N_Q=N(Q,r)$ is determined by resonant phonon absorption scattering electrons from below to above the Fermi surface (diminishing N_Q) and by resonant phonon emission by thermally excited electrons which scatter into empty states of lower energy (enhancing N_Q). To better compare with the superconducting analog, we separately treat the $(k,\uparrow)$ and the $(-k,\downarrow)$ electron processes. Then the evolution rate is

$$\frac{dN_Q}{dt}=-\frac{2\pi}{\hbar}\sum_k |M_{k,k+Q}|^2[f_k(1-f_{k+Q})N_Q-f_{k+Q}(1-f_k)(N_Q+1)]\delta(\epsilon_k-\epsilon_{k+Q}+\omega_Q)$$

$$-\frac{2\pi}{\hbar}\sum_k |M_{-k-Q,-k}|^2[f_{-k-Q}(1-f_{-k})N_Q-f_{-k}(1-f_{-k-Q})(N_Q+1)]\delta(\epsilon_{-k-Q}-\epsilon_{-k}+\omega_Q). \quad \text{(B1)}$$

Here f_k is the equilibrium electron occupancy (Fermi-Dirac distribution). It is easy to verify that when the phonon distribution is replaced on the right-hand side of Eq. (B1) by the equilibrium (Bose-Einstein) distribution n_Q, the decay rate dN_Q/dt is zero. When N_Q is written as $n_Q+\delta N_Q$, then the decay rate is $-2\gamma_Q\delta N_Q$ which defines the decay rate $2\gamma_Q=1/\tau_Q$. This in turn is -2 times the imaginary part of the phonon self-energy. Therefore we have

$$\mathrm{Im}[\Pi_N(Q,\omega)]=-\frac{\pi}{\hbar}\sum_k |M_{k,k+Q}|^2[(f_k-f_{k+Q})\delta(\epsilon_{k+Q}-\epsilon_k-\omega)+(f_{-k-Q}-f_{-k})\delta(\epsilon_{-k}-\epsilon_{-k-Q}-\omega)]$$

$$=-\frac{\pi}{\hbar}\int_{-\infty}^{\infty}d\epsilon\int_{-\infty}^{\infty}d\epsilon'\sum_k |M_{k,k+Q}|^2\delta(\epsilon_k-\epsilon)\delta(\epsilon_{k+Q}-\epsilon')$$

$$\times\{[f(\epsilon)-f(\epsilon')]\delta(\epsilon'-\epsilon-\omega)+[f(\epsilon')-f(\epsilon)]\delta(\epsilon-\epsilon'-\omega)\}. \quad \text{(B2)}$$

Two factors of $1=\int_{-\infty}^{\infty}d\epsilon\,\delta(\epsilon_k-\epsilon)$ have been inserted into this equation for subsequent convenience. Now we use the Migdal arguments[24] about the smallness of phonon energies compared to the scale on which electronic energy bands (or density of states) have any significant structure. To be specific, we are only interested in knowing the value of $\mathrm{Im}[\Pi_N(Q,\omega)]$ for energy transfers ω equal to the energies of phonon resonances. Then the factors $\delta(\epsilon-\epsilon'\pm\omega)$ tell us that ϵ and ϵ' are within $\pm\omega$ of each other, while the factors $f(\epsilon')-f(\epsilon)$ tell us that ϵ and ϵ' are on opposite sides of the Fermi energy. This means that both ϵ and ϵ' are within ω of the Fermi energy. Now consider the factor

$$A_Q(\epsilon,\epsilon')\equiv\sum_k |M_{k,k+Q}|^2\delta(\epsilon_k-\epsilon)\delta(\epsilon_{k+Q}-\epsilon'), \quad \text{(B3)}$$

which appears inside the integrals of Eq. (B2). The scale of variation of A_Q with its variables ϵ and ϵ' is the electronic energy scale ≈ 1 eV, slow compared to the rapid variation with ϵ and ϵ' of the remaining factors inside the integrals of Eq. (B2), which vanish when ϵ or ϵ' is farther than ω from the Fermi energy. Therefore, $A_Q(\epsilon,\epsilon')$ can be replaced by $A_Q(0,0)$, its value when both electron energies are held at the Fermi energy. The integrals over ϵ and ϵ' can now be done exactly, and Eq. (B2) can be written as Eq. (A4), with γ_Q given by

$$\gamma_Q=\frac{2\pi}{\hbar}\omega_Q\sum_k |M_{k,k+Q}|^2\delta(\epsilon_k)\delta(\epsilon_{k+Q}). \quad \text{(B4)}$$

In common with other related Migdal arguments,[24] the corrections to this expression are governed by the small parameter $N(0)\hbar\omega$.

APPENDIX C: PHONON DECAY IN THE SUPERCONDUCTING STATE

To include superconductivity using Eq. (A1), it is proper to use Eliashberg theory.[25] Instead, we assume that the interactions which cause superconductivity (not necessarily phonons) can be treated as a separate added BCS ''reduced'' interaction. Making the usual Bogoliubov-Valatin transformation ($\gamma_k=u_k c_{k\uparrow}-v_k c^\dagger_{-k\downarrow}$), the Hamiltonian Eq. (A1) becomes[25]

$$H=\sum_k E_k(\gamma^\dagger_{k\uparrow}\gamma_{k\uparrow}+\gamma^\dagger_{-k\downarrow}\gamma_{-k\downarrow})+\sum_Q \omega_Q a^\dagger_Q a_Q$$

$$+\sum_{k,Q} M_{k,k+Q}(a_Q+a^\dagger_{-Q})[n_{k,k+Q}(\gamma^\dagger_{k+Q\uparrow}\gamma_{k\uparrow}$$

$$+\gamma^\dagger_{-k\downarrow}\gamma_{-k-Q\downarrow})+m_{k,k+Q}(\gamma^\dagger_{k+Q\uparrow}\gamma^\dagger_{-k\downarrow}-\gamma_{k\uparrow}\gamma_{-k-Q\downarrow})], \quad \text{(C1)}$$

where E_k is the BCS quasiparticle energy $\sqrt{(\epsilon_k^2+\Delta^2)}$, and n and m are BCS ''coherence factors,''

$$(n_{k,k+Q})^2=\frac{1}{2}\left(1+\frac{\epsilon_k\epsilon_{k+Q}-\Delta^2}{E_kE_{k+Q}}\right), \quad \text{(C2)}$$

$$(m_{k,k+Q})^2=\frac{1}{2}\left(1-\frac{\epsilon_k\epsilon_{k+Q}-\Delta^2}{E_kE_{k+Q}}\right). \quad \text{(C3)}$$

Just as in the N state, we now imagine that the phonon occupation numbers N_Q are driven out of equilibrium, and construct the evolution equation, setting dN_Q/dt equal to $-2\gamma_Q^S\delta N_Q$. The result gives the imaginary part of the S-state phonon self-energy

$$-\mathrm{Im}[\Pi_S(Q,\omega)] = \frac{\pi}{\hbar}\sum_k |M_{k,k+Q}|^2\{n^2_{k,k+Q}[(f_k - f_{k+Q})\,\delta(E_{k+Q}-E_k-\omega)+(f_{-k-Q}-f_{-k})\,\delta(E_{-k}-E_{-k-Q}-\omega)]$$
$$+ m^2_{k,k+Q}[(1-f_{-k}-f_{k+Q})\,\delta(E_{k+Q}+E_{-k}-\omega)-(1-f_{-k-Q}-f_k)\,\delta(E_k+E_{-k-Q}+\omega)]\}. \quad \text{(C4)}$$

Here the Fermi equilibrium occupation function f_k is for superconducting quasiparticles with energy E_k. When T exceeds T_c, this formula correctly reduces to Eq. (B2). Now we again use the Migdal arguments, which lead to a simplified formula, given as Eq. (2) of the text, for the case $\omega > 0$.

[1] H. Kawano, H. Yoshizawa, H. Takeya, and K. Kadowaki, Phys. Rev. Lett. **77**, 4628 (1996).
[2] C. Stassis, M. Bullock, J. Zarestky, P. Canfield, A. I. Goldman, G. Shirane, and S. M. Shapiro, Phys. Rev. B **55**, R8678 (1997).
[3] S. M. Shapiro, G. Shirane, and J. D. Axe, Phys. Rev. B **12**, 4899 (1975).
[4] H. A. Mook, B. C. Chakoumakos, M. Mostoller, A. T. Boothroyd, and D. McK. Paul, Phys. Rev. Lett. **69**, 2272 (1992).
[5] N. Pyka, W. Reichardt, L. Pintschovius, G. Engel, J. Rossat-Mignod, and J. Y. Henry, Phys. Rev. Lett. **70**, 1457 (1993).
[6] C. Thomsen, in *Light Scattering in Solids VI*, edited by by M. Cardona and G. Güntherodt (Springer-Verlag, Heidelberg, 1991), p. 285.
[7] B. Friedl, C. Thomsen, and M. Cardona, Phys. Rev. Lett. **65**, 915 (1990).
[8] A. P. Litvinchuk, C. Thomsen, and M. Cardona, Solid State Commun. **80**, 257 (1991).
[9] E. Altendorf, J. Chrzanowski, J. C. Irwin, A. O'Reilly, and W. N. Hardy, Physica C **175**, 47 (1991).
[10] M. V. Klein and S. B. Dierker, Phys. Rev. B **29**, 4976 (1984).
[11] R. Zeyher and G. Zwicknagl, Z. Phys. B **78**, 175 (1990).
[12] H.-Y. Kee and C. M. Varma (unpublished).
[13] H. G. Schuster, Solid State Commun. **13**, 1559 (1973).
[14] R. Zeyher, Phys. Rev. B **44**, 9596 (1991).
[15] J. R. Clem, Ann. Phys. (N.Y.) **40**, 268 (1966).
[16] F. Marsiglio, Phys. Rev. B **47**, 5419 (1993).
[17] P. B. Allen, in *Dynamical Properties of Solids*, edited by G. K. Horton and A. A. Maradudin (North-Holland, Amsterdam, 1980), Vol. 3, p. 95.
[18] W. E. Pickett and D. J. Singh, Phys. Rev. Lett. **72**, 3702 (1994); L.F. Mattheiss, Phys. Rev. B **49**, 13 279 (1994); R. Coehoorn, Physica C **228**, 331 (1994).
[19] W. H. Butler, H. G. Smith, and N. Wakabayashi, Phys. Rev. Lett. **39**, 1004 (1977).
[20] T. Ekino, H. Fujii, M. Kosugi, Y. Zenitani, and J. Akimitsu, Physica C **235-240**, 2529 (1994).
[21] A. Andreone, F. Fontana, M. Iavarone, R. Vaglio, F. Canepa, P. Manfrinetti, and A. Palenzona, Physica C **251**, 379 (1995).
[22] G. T. Jeong, J. I. Kye, S. H. Chun, Z. G. Khim, W. C. Lee, P. C. Canfield, B. K. Cho, and D. C. Johnston, Physica C **253**, 48 (1995).
[23] F. Bommeli, L. Degiorgi, P. Wachter, B. K. Cho, P. C. Canfield, R. Chau, and M. B. Maple, Phys. Rev. Lett. **78**, 547 (1997).
[24] P. B. Allen and B. Mitrović, in *Solid State Physics: Advances in Research and Applications*, edited by F. Seitz, D. Turnbull, and H. Ehrenreich (Academic, New York, 1982), Vol. 37, pp. 1–92; see especially pp. 17 and 22ff.
[25] J. R. Schrieffer, *Theory of Superconductivity* (Benjamin, New York, 1964); p. 62ff.